MODEL UPDATING OF DYNAMICALLY TIME LINEAR REDUCED ORDER MODELS

Laurence M. Griffiths[1], Dorian P. Jones[1], and Michael I. Friswell[2]

[1]University of Bristol
Department of aerospace Engineering, University of Bristol, Bs8 1TR, UK
laurence.griffiths@bristol.ac.uk, dorian.jones@bristol.ac.uk

[2]Swansea University
School of Engineering, Swansea University, Singleton Park, Swansea SA2 8PP, UK
M.I.Friswell@swansea.ac.uk

Abstract: Here we present a novel approach to applying model updating to reduced order models (ROM) of computational fluid dynamics (CFD) codes. Differences in the boundary conditions and simplifications to the model often mean the steady state behaviour of the the underlying CFD scheme is incorrectly identified. By updating both the steady state magnitude and gradient of the ROM from higher order CFD or experimental data we can reduce these discrepancies. In this paper we present results of model updating of an unsteady aerofoil in an internal flow to a free flight condition.

1 INTRODUCTION

Across all engineering disciplines, the differences found between experimental results and computational simulations gives rise to various degrees of uncertainty in the solutions. In fluid dynamics these differences can be broadly split into issues of boundary conditions and numerical accuracy. Within the computational fluid dynamics (CFD) community a great deal of effort has been invested in reducing numerical error, yet large discrepancies with experimental data still persist. The nature of experimental and computational studies often dictates the application of different boundary conditions applied in each. Furthermore, for aerospace applications it is often the case that both experimental and computational methods are attempting to model a free flying aircraft but doing so by applying fundamentally different conditions. Model updating provides the opportunity to modify the behaviour of the system to reduce these discrepancies.

In structural dynamics particularly, model updating is a well established and successful field, especially in solving the finite element equations [1, 2] . In this research we develop a novel method of applying model updating to reduced order models (ROM) of a aerodynamic simulations.

The reduced order modelling procedure applied here is a dynamically time linear single input single output (SISO) model constructed about a nonlinear flow solution. A modification to the input and output matrices of the system allows for an updated steady state gradient. Essentially we now construct a reduced order model of a system with a chosen steady state slope and magnitude.

2 THEORY

2.1 CFD MODEL

The CFD code used is a modified Jameson cell centred finite volume scheme for the solution of the Euler equations on a moving mesh [3–5].

The Euler equations can be expressed as a nonlinear state space formulation:

$$\begin{aligned} \frac{\partial \mathbf{x}(t)}{\partial t} &= \mathbf{f}(t, \mathbf{x}(t), \mathbf{u}(t)) \\ \mathbf{y}(t) &= \mathbf{h}(t, \mathbf{x}(t), \mathbf{u}(t)) \end{aligned} \tag{1}$$

where for an aerofoil with pitch, heave and flap motion:

$$\mathbf{u} = \begin{bmatrix} \alpha \\ \dot{\alpha} \\ h \\ \dot{h} \\ \delta \\ \dot{\delta} \end{bmatrix}, \quad \mathbf{x} = \begin{bmatrix} \rho_{1,1} \\ \rho u_{1,1} \\ \rho v_{1,1} \\ e_{1,1} \\ \vdots \\ \rho_{imax,jmax} \\ \rho u_{imax,jmax} \\ \rho v_{imax,jmax} \\ e_{imax,jmax} \end{bmatrix}, \quad \mathbf{y} = \begin{bmatrix} C_l \\ C_d \\ C_m \\ C_h \end{bmatrix} \tag{2}$$

Note that the application of the ERA means that the Euler equations need never be explicitly expressed in their state space form, and a standard solver can be used.

2.2 Linear State space representation

When constructing the reduced order model we assume that the unsteady response about the nonlinear mean is linear. This allows (1) to be represented as a continuous linear state space model:

$$\begin{aligned} \frac{\partial \mathbf{x}(t)}{\partial t} &= \mathbf{A}\mathbf{x}(t) + \mathbf{B}\mathbf{u}(t) \\ \mathbf{y}(t) &= \mathbf{C}\mathbf{x}(t) + \mathbf{D}\mathbf{u}(t) \end{aligned} \tag{3}$$

which for an implicit CFD scheme can be discretised as

$$\begin{aligned} \frac{\mathbf{x}_k - \mathbf{x}_{k-1}}{\Delta t} &= \mathbf{A}\mathbf{x}_k + \mathbf{B}\mathbf{u}_k \\ \mathbf{y}_k &= \mathbf{C}\mathbf{x}_k + \mathbf{D}\mathbf{u}_k \end{aligned} \tag{4}$$

upon rearranging yields

$$\begin{aligned} \mathbf{x}_k &= (I - \Delta t\mathbf{A})^{-1}\mathbf{x}_{k-1} + (I - \Delta t\mathbf{A})^{-1}\Delta t\mathbf{B}\mathbf{u}_k \\ \mathbf{y}_k &= \mathbf{C}\mathbf{x}_k + \mathbf{D}\mathbf{u}_k \end{aligned} \tag{5}$$

if we let

$$\begin{aligned} \tilde{\mathbf{A}} &= (\mathbf{I} - \Delta t\mathbf{A})^{-1} \\ \tilde{\mathbf{B}} &= (\mathbf{I} - \Delta t\mathbf{A})^{-1}\mathbf{B}\Delta t \\ \tilde{\mathbf{C}} &= \mathbf{C} \\ \tilde{\mathbf{D}} &= \mathbf{D} \end{aligned} \tag{6}$$

then the discrete system becomes:

$$\begin{aligned} \mathbf{x}_k &= \tilde{\mathbf{A}}\mathbf{x}_{k-1} + \tilde{\mathbf{B}}\mathbf{u}_k \\ \mathbf{y}_k &= \tilde{\mathbf{C}}\mathbf{x}_k + \tilde{\mathbf{D}}\mathbf{u}_k \end{aligned} \tag{7}$$

2.3 System Identification and reduction

Using the Eigenvalue Realisation Algorithm (ERA) of Juang and Pappa [6] we can identify the discrete system matrices $\tilde{\mathbf{A}}, \tilde{\mathbf{B}}, \tilde{\mathbf{C}}$ given the pulse response $\mathbf{y}(t)$ of the CFD code. A linearised form of the Euler equations [7] have been used to calculate the unsteady pulse response. It is also possible to use a nonlinear Euler code for the pulse response and then extract the linear component by applying Volterra theory [8]. Here only the brief overview of the application of the ERA is given, for a more in depth discussion see Jones and Gaitonde [9].

The method of Juang and Pappa requires the generation of the generalised Hankel matrix:

$$\mathbf{H}^{rs}(k) = \begin{bmatrix} \mathbf{H}_k & \mathbf{H}_{k+1} & \mathbf{H}_{k+2} & \cdots & \mathbf{H}_{k+s-1} \\ \mathbf{H}_{k+1} & \mathbf{H}_{k+2} & \mathbf{H}_{k+3} & \cdots & \mathbf{H}_{k+s} \\ \vdots & \vdots & \vdots & \ddots & \vdots \\ \mathbf{H}_{k+r-1} & \mathbf{H}_{k+r} & \mathbf{H}_{k+r+1} & \cdots & \mathbf{H}_{k+s+r-2} \end{bmatrix}$$
$$= \begin{bmatrix} \tilde{\mathbf{C}}\tilde{\mathbf{A}}^{k}\tilde{\mathbf{B}} & \tilde{\mathbf{C}}\tilde{\mathbf{A}}^{k+1}\tilde{\mathbf{B}} & \tilde{\mathbf{C}}\tilde{\mathbf{A}}^{k+2}\tilde{\mathbf{B}} & \cdots & \tilde{\mathbf{C}}\tilde{\mathbf{A}}^{k+s-1}\tilde{\mathbf{B}} \\ \tilde{\mathbf{C}}\tilde{\mathbf{A}}^{k+1}\tilde{\mathbf{B}} & \tilde{\mathbf{C}}\tilde{\mathbf{A}}^{k+2}\tilde{\mathbf{B}} & \tilde{\mathbf{C}}\tilde{\mathbf{A}}^{k+3}\tilde{\mathbf{B}} & \cdots & \tilde{\mathbf{C}}\tilde{\mathbf{A}}^{k+s}\tilde{\mathbf{B}} \\ \vdots & \vdots & \vdots & \ddots & \vdots \\ \tilde{\mathbf{C}}\tilde{\mathbf{A}}^{k+r-1}\tilde{\mathbf{B}} & \tilde{\mathbf{C}}\tilde{\mathbf{A}}^{k+r}\tilde{\mathbf{B}} & \tilde{\mathbf{C}}\tilde{\mathbf{A}}^{k+r+1}\tilde{\mathbf{B}} & \cdots & \tilde{\mathbf{C}}\tilde{\mathbf{A}}^{k+s+r-2}\tilde{\mathbf{B}} \end{bmatrix} \quad (8)$$

where the rows and columns of the matrix $\mathbf{H}^{rs}(k)$ are the unit sample response of the CFD scheme to a perturbation on each input channel. For each input channel of $\mathbf{u}_i$ of the CFD scheme the impulse response is taken with all other input channels set to zero $\mathbf{u}_{n\neq i} = 0$. The ROMs used here are single input single output, so from the pulse responses of each input channel $\mathbf{u}$ we can construct a ROM for each input-output pair of the CFD scheme. Eqn. (3) now become:

$$\begin{aligned} \frac{\partial\, \mathbf{x}|_{ij}(t)}{\partial t} &= \mathbf{A}|_{ij}\, \mathbf{x}|_{ij}(t) + \mathbf{B}|_{ij} u_i(t) \\ y_j|_i(t) &= \mathbf{C}|_{ij}\, \mathbf{x}|_{ij}(t) + D|_{ij}\, u_i(t) \end{aligned} \quad (9)$$

where $\mathbf{u}_i$ is a scalar variable for i^{th} input, $\mathbf{y}_j|_i$ is a scalar for the j^{th} output of the system evaluated for the i^{th} input. $\mathbf{A}|_{ij}$, $\mathbf{B}|_{ij}$ $\mathbf{C}|_{ij}$ and $\mathbf{D}|_{ij}$ are the system matrices evaluated for the i^{th} input and j^{th} output. For ease of notation the subscripts i, j will be implied. The realisation applied here is balanced, meaning that the rank of the input/out matrices $\mathbf{A}$ and $\mathbf{B}$ are of equal rank, consequently $\mathbf{A}$ because a square matrix. The dimensions of the system are:

$$\mathbf{A}|_{ij} = \begin{bmatrix} \vdots & \\ \cdots & n \times n \quad \cdots \\ \vdots & \end{bmatrix} \qquad \mathbf{B}|_{ij} = \begin{bmatrix} \vdots \\ n \times 1 \\ \vdots \end{bmatrix} \qquad \mathbf{C}|_{ij} = \begin{bmatrix} \cdots & 1 \times n & \cdots \end{bmatrix}$$

$$y_j|_i = \begin{bmatrix} 1 \times 1 \end{bmatrix} \qquad u_i = \begin{bmatrix} 1 \times 1 \end{bmatrix} \qquad \mathbf{x}|_{ij} = \begin{bmatrix} \vdots \\ n \times 1 \\ \vdots \end{bmatrix} \qquad D|_{ij} = \begin{bmatrix} 1 \times 1 \end{bmatrix}$$

In practise a pulse input magnitude of less than unity is required to prevent breakdown and poorly converged solutions of the CFD model. The required pulse magnitude can be

estimated by applying a local 1D piston theory [10] prior to running the CFD. The pulse response is then rescaled to yield an equivalent unit response.

2.4 Reduced order model updating

If the steady state gradient of the nonlinear mean flow solution is inconsistent with a target system then the steady state error will carry through into the identified ROM. In the following chapter we will discuss a method by which the steady state behaviour of the ROM can be updated.

The steady state gradient $\partial y_j/\partial u_i$ of the of the ROM identified in Eqn. 7 can be identified from a step input to the system in the limit $t \to \infty$, where t is the nondimensional time. Let us consider a step down response of the ROM, going from a perturbed state $u = 1$ for $t \leq 0$, returning to the mean solution $u = 0$ at $t = 1$ (Fig. 1). For this response, the system output y_i will return to the nonlinear mean flow solution in the limit $t \to \infty$.

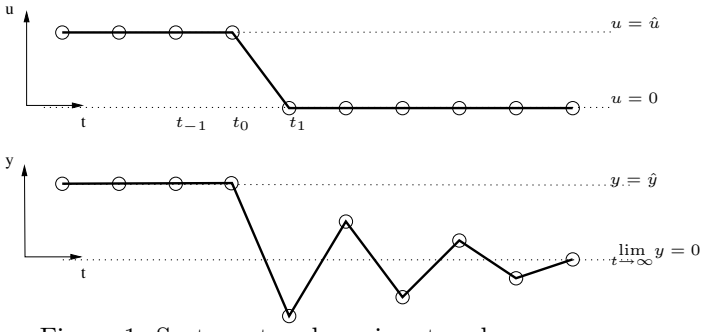

Figure 1: System step-down input and response

As the linear system is expressed as a perturbation from the nonlinear mean then the steady state gradient becomes:

$$\frac{\partial \hat{y}}{\partial \hat{u}} = \frac{\hat{y}}{\hat{u}}$$

substituting the following boundary conditions for $t \leq 0$ into the linear state space system(4)

$$x_{t<0} = x_{t=0} \qquad u_{t\leq 0} = \hat{u}$$

gives

$$\hat{\mathbf{x}} = -\mathbf{A}^{-1}\mathbf{B}\hat{u} \tag{10}$$

$$\frac{\hat{\mathrm{y}}}{\hat{u}} = -\mathbf{C}\mathbf{A}^{-1}\mathbf{B} + D \tag{11}$$

taking the eigenvalue decomposition of $\mathbf{A}$ such that $\mathbf{A} = \mathbf{Q}\mathbf{\Lambda}\mathbf{Q}^{-1}$

$$\frac{\hat{\mathrm{y}}}{\hat{u}} = -\mathbf{C}\mathbf{Q}\mathbf{\Lambda}^{-1}\mathbf{Q}^{-1}\mathbf{B} + D = -\mathbf{C}_Q\mathbf{\Lambda}^{-1}\mathbf{B}_Q + D \tag{12}$$

letting

$$\begin{aligned} \mathbf{A}_Q &= \mathbf{\Lambda} \\ \mathbf{B}_Q &= \mathbf{Q}^{-1}\mathbf{B} \\ \mathbf{C}_Q &= \mathbf{C}\mathbf{Q} \end{aligned} \tag{13}$$

if the gradient $\partial\hat{y}/\partial\hat{u}$ is inconsistent with that of our target system (such as higher order CFD or experimental methods), then we can update the gradient:

$$\frac{\hat{\mathrm{y}}}{\hat{u}} + \epsilon = -(\mathbf{C}_Q + \mathbf{E})\mathbf{\Lambda}^{-1}(\mathbf{B}_Q + \mathbf{E}^T) + D \tag{14}$$

where

$$\mathbf{E} = \mathbf{E}_\sigma \sigma \tag{15}$$

here σ is the scalar update parameter. $\mathbf{E}_\sigma$ is a chosen weighting sequence of σ on each of the eigenvalues values of the system matrix $\mathbf{A}$, i.e. the diagonal entries of $\mathbf{\Lambda}$. Rearranging (14) and subtracting (11) yields:

$$\sigma^2 \left[\mathbf{E}_\sigma \mathbf{\Lambda}^{-1} \mathbf{E}_\sigma^T\right] + \sigma \left[\mathbf{B}_Q \mathbf{\Lambda}^{-1} \mathbf{E}_\sigma^T + \mathbf{E}_\sigma \mathbf{\Lambda}^{-1} \mathbf{C}_Q\right] + \epsilon = 0 \tag{16}$$

such that σ is now the solution of a scalar quadratic. In discrete space Eqn. (14) and (16) can be expressed as:

$$\frac{\hat{\mathrm{y}}}{\hat{u}} + \epsilon = (\tilde{\mathbf{C}}_Q + \tilde{\mathbf{E}}) \left(\mathbf{I} - \tilde{\mathbf{\Lambda}}\right)^{-1} (\tilde{\mathbf{B}}_Q + \tilde{\mathbf{E}}^T) + D \tag{17}$$

and

$$\sigma^2 \left[\tilde{\mathbf{E}}_\sigma \left(\mathbf{I} - \tilde{\mathbf{\Lambda}}\right)^{-1} \tilde{\mathbf{E}}_\sigma^T\right] + \sigma \left[\tilde{\mathbf{B}}_Q \left(\mathbf{I} - \tilde{\mathbf{\Lambda}}\right)^{-1} \tilde{\mathbf{E}}_\sigma^T + \tilde{\mathbf{E}}_\sigma \left(\mathbf{I} - \tilde{\mathbf{\Lambda}}\right)^{-1} \tilde{\mathbf{C}}_Q\right] - \epsilon = 0 \tag{18}$$

2.5 Setting the update weighting sequence

We can set the weighting sequence $\mathbf{E}_\sigma$ of the update parameter σ as a function of the eigenvalues of the system matrix $\mathbf{A}$. From Eqn (14) the steady state update can be expressed as a summation across the inverse of each eigenvalue of $\mathbf{A}$ and the corresponding input/out matrices $\mathbf{B}_Q$ and $\mathbf{C}_Q$. The weighting sequence $\mathbf{E}_\sigma$ can be used to isolate the update onto the response corresponding to a chosen set of eigenvalues of the linear system.

Fig. (2) shows a typical distribution of eigenvalues from ROM to the pulse input of a CFD scheme.

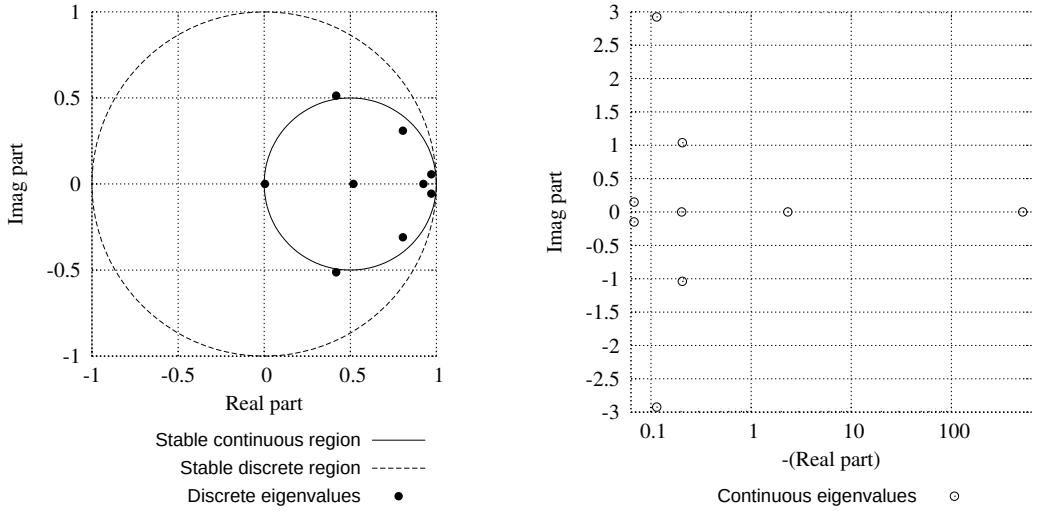

Figure 2: Typical eigenvalue plots

The frequency and damping ratio of each of the eigenvalues in real (continuous) space is expressed as:

$$\begin{aligned} \omega_n &= \sqrt{\Lambda_{real}^2 + \Lambda_{imag}^2} \\ \zeta &= \frac{\Lambda_{real}}{\sqrt{\Lambda_{real}^2 + \Lambda_{imag}^2}} \end{aligned} \tag{19}$$

where Λ is the continuous time eigenvalue, ω_n is the natural frequency, and ζ is the corresponding damping ratio of the eigenvalue. The continuous time eigenvalues can be related to the discrete implicit system eigenvalues $\tilde{\Lambda}$ by:

$$\Lambda = \frac{1 - \tilde{\Lambda}}{\tilde{\Lambda}\Delta t} \tag{20}$$

Initial research has shown that, in continuous space the smallest real eigenvalue corresponds to the immediate CFD response after the initial time step. The eigenvalue closest to $\Lambda = 0 + 0i$ has a lesser effect on the immediate transient, but has a greater impact on the long term steady state behaviour of the response. Even though the magnitudes and distributions of the eigenvalues will be case dependant, there should always be a mode (or pair of complex conjugate modes) corresponding to the immediate high frequency and the the long term low frequency responses.

The solution to (16) provides two possible roots σ. The smallest root has always been chosen as this provides to the smallest perturbation from the existing response to the target solution.

3 INTERNAL-EXTERNAL FLOW UPDATING

Updating a reduced order model is not limited to any specific case. Here however we present an example of updating an internal flow to a target external flow. The intention

here is to show an example and initial results of model updating for ROMs. In the next section we will provide details of problems encountered while producing these results.

The results presented here are for a NACA 0012 aerofoil pitching about the quarter chord. The tunnel walls have been included as a symmetry plane. All the meshes are 251 x 40 cells with 201 cells over the aerofoil and a first cell height of 0.003c (Fig. 4-3). The nonlinear mean flow solutions about which the ROM is constructed are shown in Fig. 6 . An overview of the test cases is given in Table 1. In all the cases, the aerofoil is undergoing a linear sinusoidal pitching motion described in dimensional variables by:

$$\alpha(t) = \alpha_{max} sin(\omega t^{dim}) \tag{21}$$

where ω is the dimensional frequency, which can be related to the reduced frequency κ as:

$$\kappa = \frac{\omega c}{2U_\infty} \tag{22}$$

Fig. 8-10 show the integral force responses to the sinusoidal pitch input. Responses have been included for updates of both the steady state gradients as given by For the steady state magnitude updates the unsteady mean flow magnitudes for the integral forces have been replaced by those from the target solution, i.e. for C_L the update would be:

$$C_L(t) = \overline{C}_L^{Target} + \Delta C_L^{Tunnel}$$

where $C_L(t)$ is the updated lift coefficient, $\overline{C}_L^{Target}$ is the nonlinear mean target lift coefficient and ΔC_L^{Tunnel} is the perturbed lift coefficient calculated from the tunnel simulation.

Test case 1 (Fig. 7) shows model updating for an unfavourable small tunnel height of 2.25c. The change in shock location from 0.4c to 0.7c explains the large differences between the internal baseline solution and the freestream. Clearly here applying a constant shift to update the steady state magnitude alone is insufficient. By updating the gradient however provides a good representation of the target solution despite the significant differences in the unsteady mean flow. Test cases 2-4 show the response from a more practical tunnel height of 9c. As the frequency of oscillation is reduced, the aerodynamic response tends to the steady state in the limit $\omega \to 0$ conversely as the frequency is increased, the impact of the steady state gradients on the frequency response are reduced as the flow becomes increasingly more governed by the high frequency eigenmodes of the system (Fig. 8-10).

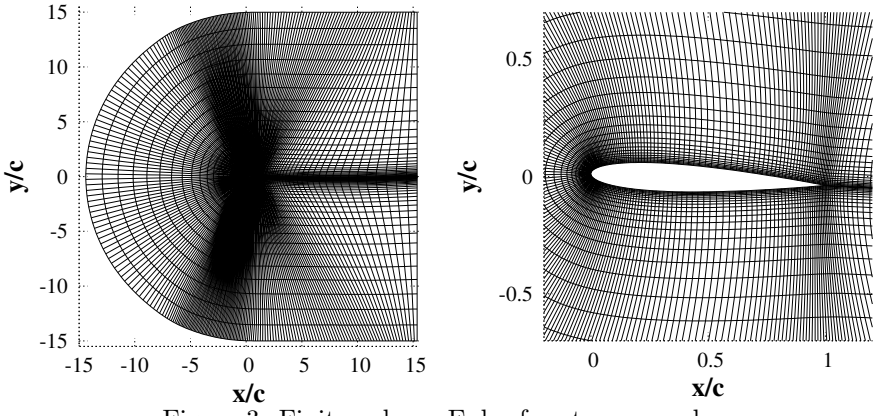

Figure 3: Finite volume Euler freestream mesh.

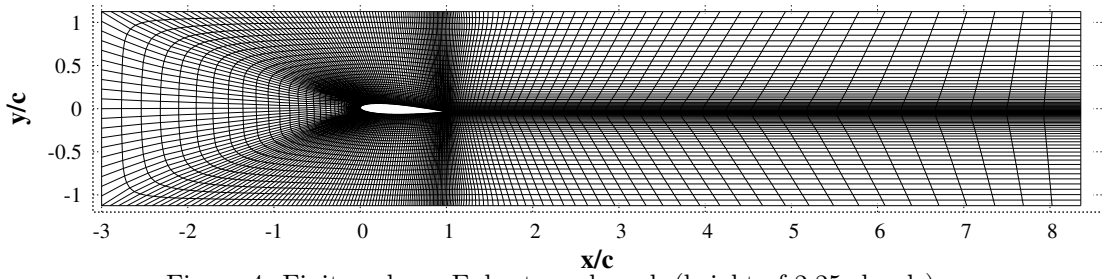

Figure 4: Finite volume Euler tunnel mesh (height of 2.25 chords).

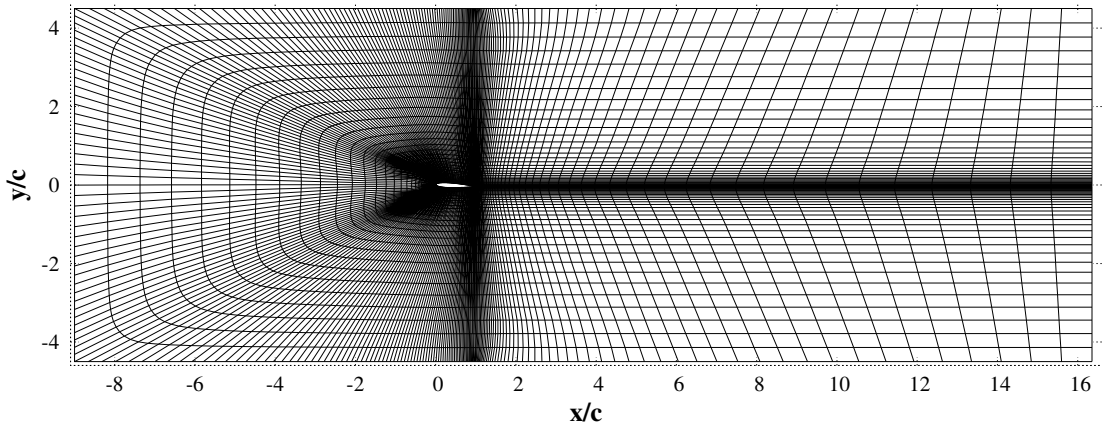

Figure 5: Finite volume Euler tunnel mesh (height of 9chord).

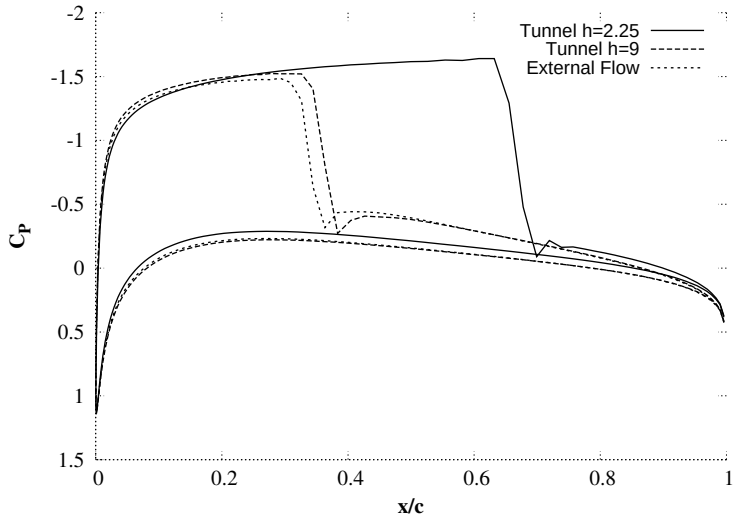

Figure 6: Nonlinear mean flow solutions

Case	κ	h	Ma	α_{mean}	α_{max}
1	0.0808	2.25c	0.7	2.89	1.0
2	0.0404	9c	0.7	2.89	1.0
3	0.0808	9c	0.7	2.89	1.0
4	0.1616	9c	0.7	2.89	1.0

Table 1: Test Cases

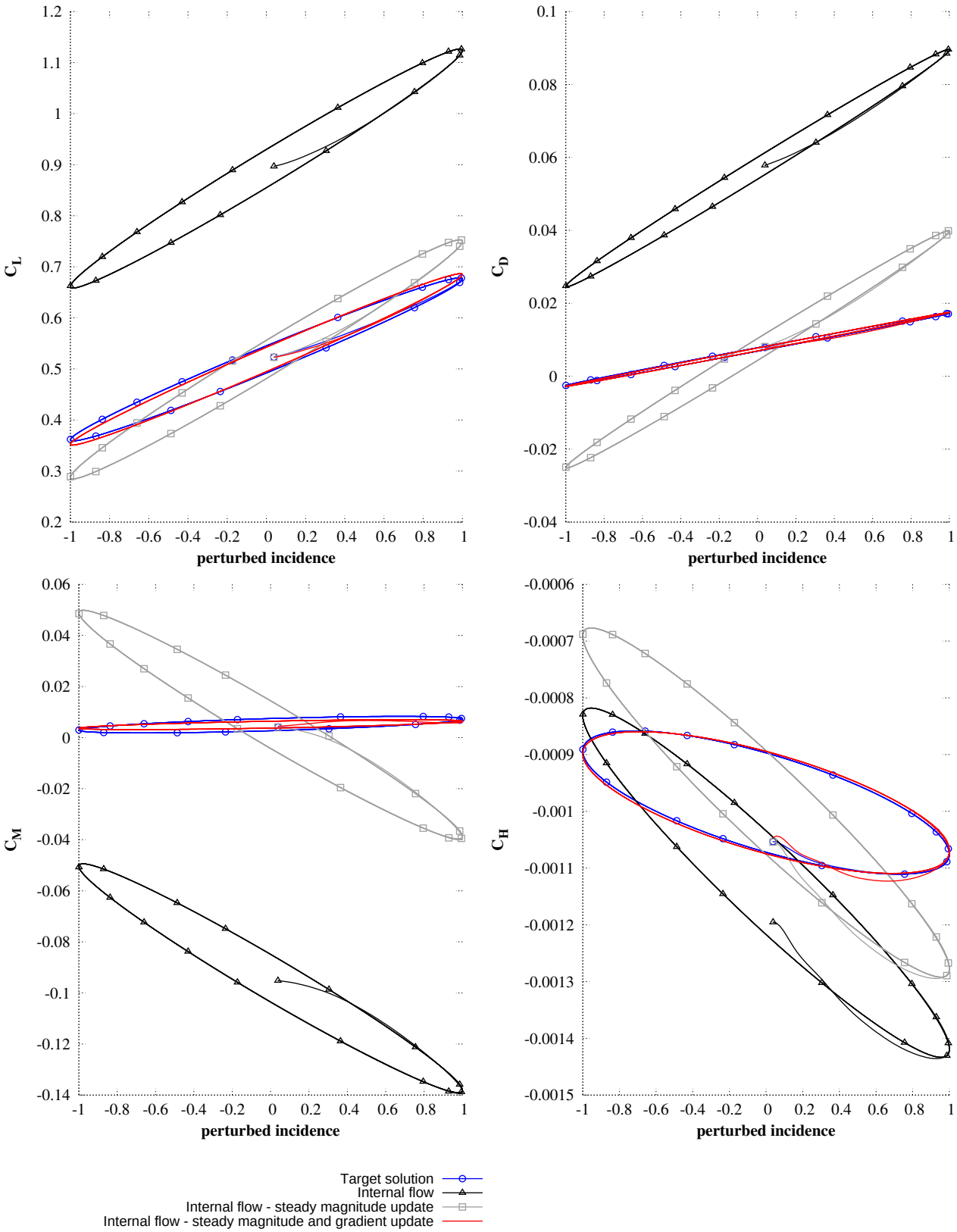

Figure 7: Test case 1- Integral force response ($\kappa = 0.0808$)

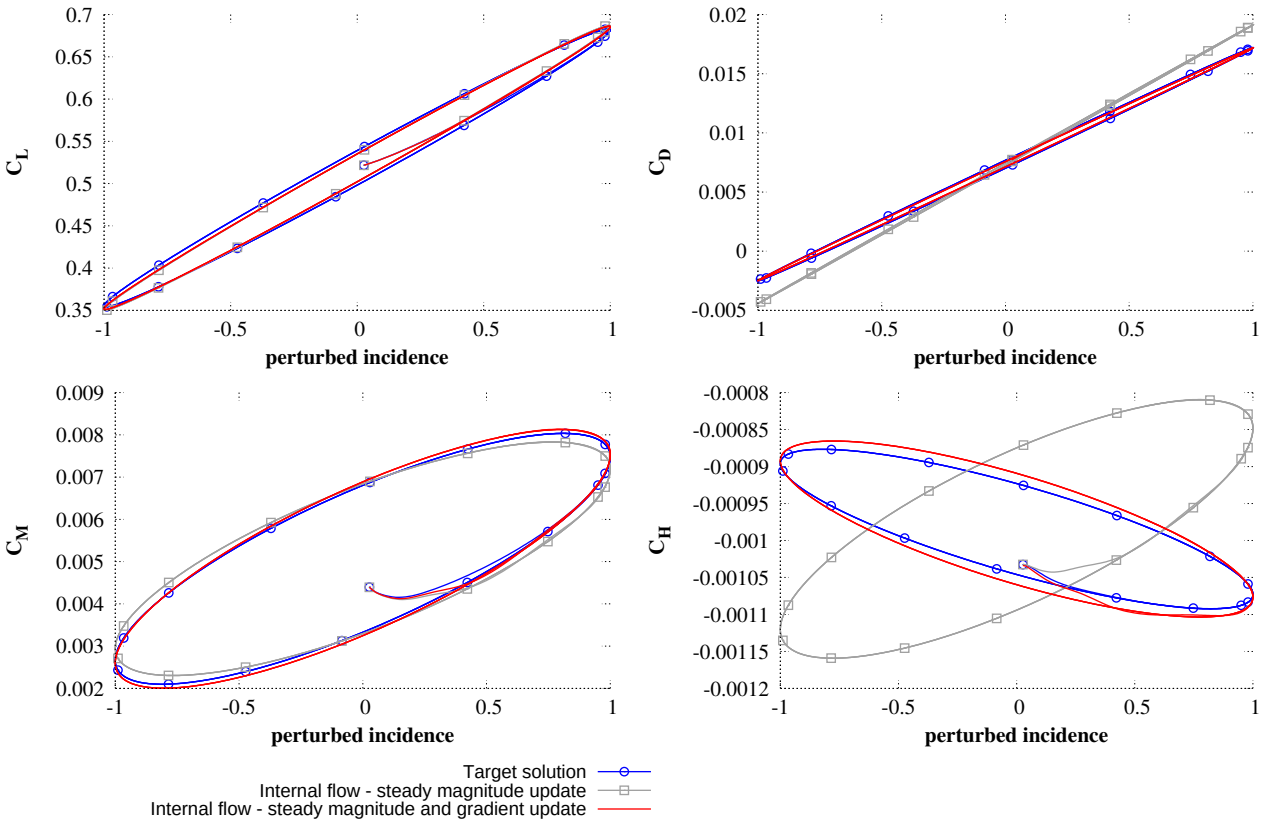

Figure 8: Test Case 2 - Integral force response ($\kappa = 0.0404$)

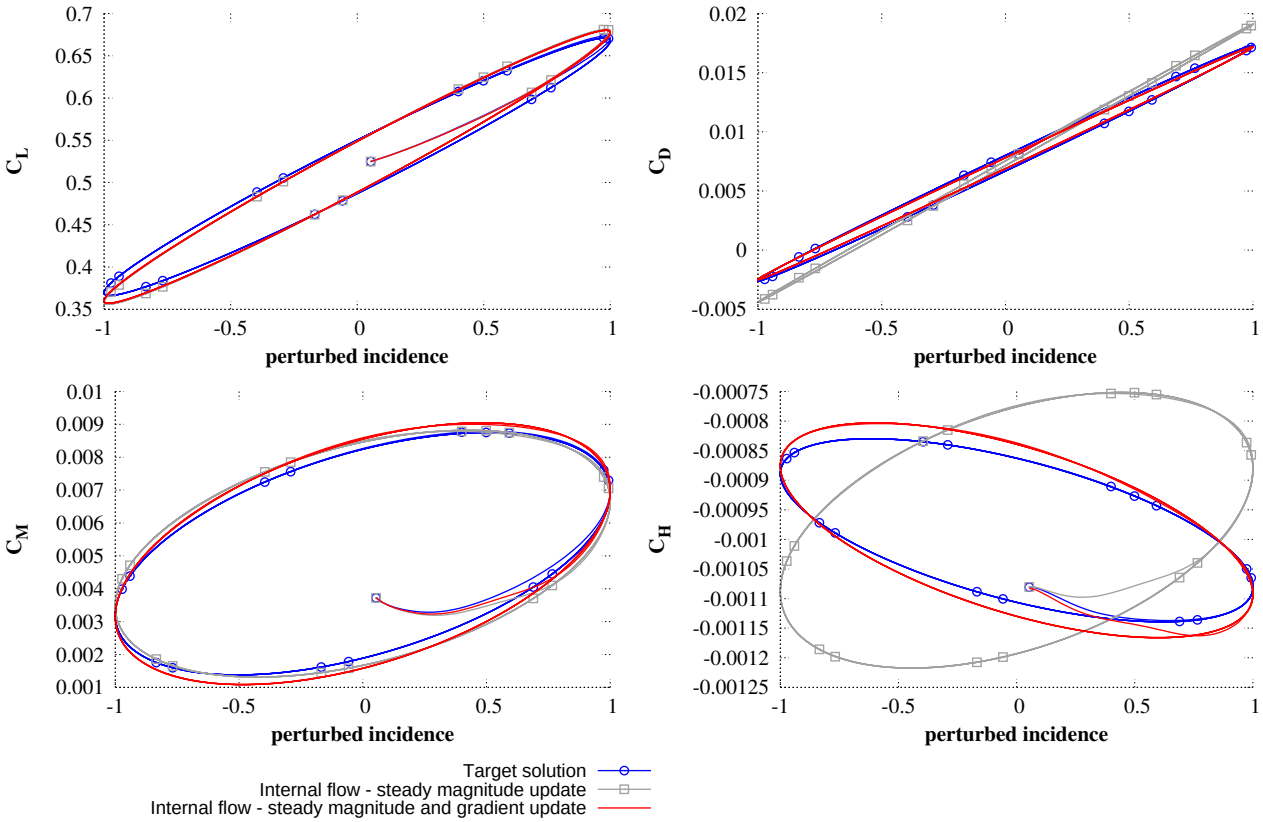

Figure 9: Test Case 3 - Integral force response ($\kappa = 0.0808$)

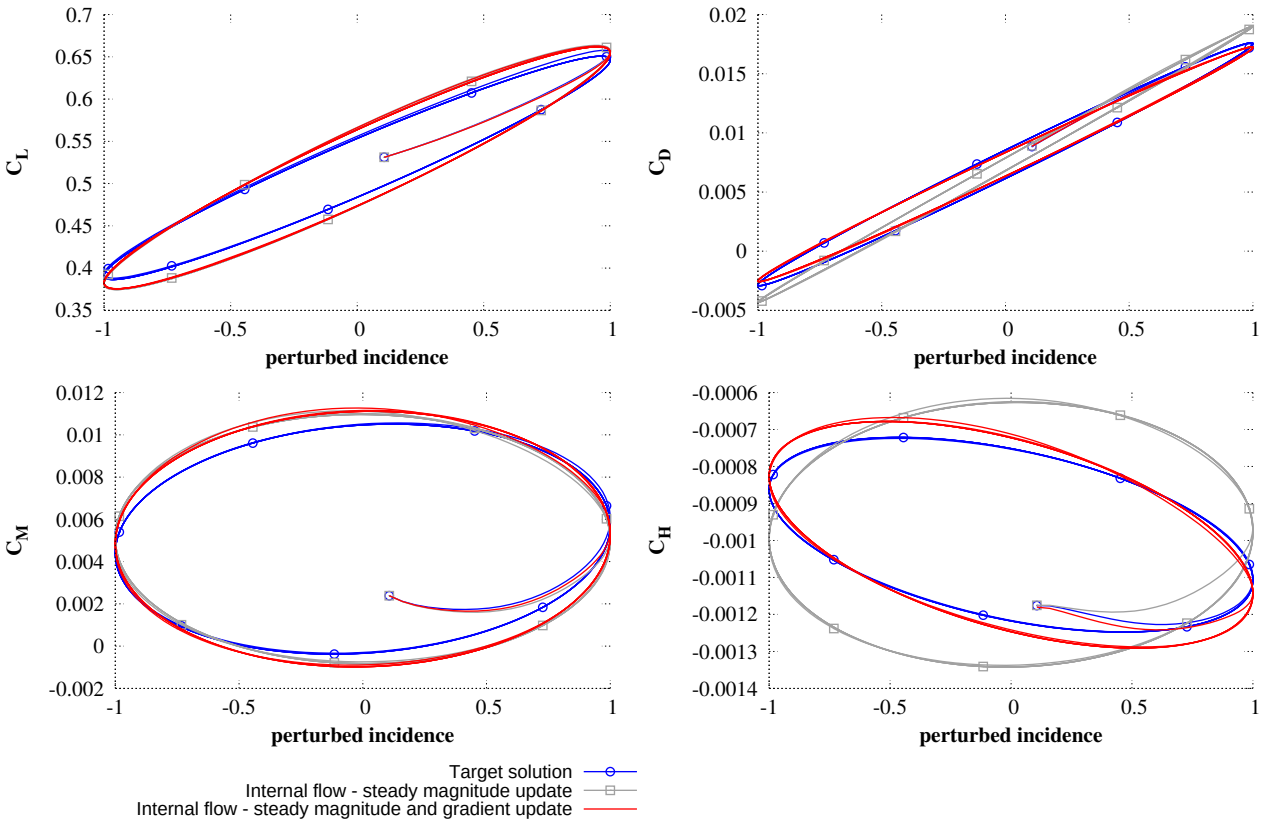

Figure 10: Test Case 4 - Integral force response ($\kappa = 0.1616$)

4 PROBLEMS ENCOUNTERED WITH UPDATING

In this section we present the initial problems encountered when applying the model updating as presented in the previous sections.

4.0.1 Real modes close to zero

The system identification can at times place an eigenvalue close to the origin $\Lambda = 0 + 0i$ in real space or $\tilde{\Lambda} = 1 + 0i$ in discrete space. This mode is almost neutrally damped, so will, with respect to any practical time scales, reach steady state in the limit $t \to \infty$.

When we update a system the solution to (16) is solved in the limit $t \to \infty$. Hence, when this mode is present, the solution is correct however impractical in as far as that for typical timescales encountered in aeroelastics the required steady state will never be reached. As this behaviour is not present in the full CFD (due to numerical and/or physical damping) then this mode can only be introduced through the system identification.

By applying a method of ROM restarting [11]an equivalent system can be identified where the selected eigenvalue has been removed. Fig. 12-11 show an example system where this mode is present. The results are generated for a RAE 2822 aerofoil pitching about the quarter chord. The tunnel has a height of 4.5c and is modelled with a mesh size of 251x40 cells with 201 cells over the aerofoil. To demonstrate the behaviour of this mode, hinge

moment responses to a step input ($\alpha = 0.5^o$) and a sinusoidal pitching motion (21) have been used.

The eigenvalues of the system before and after the removal of the eigenvalue $\tilde{\Lambda} = 0.9997 + 0i$ are shown in Fig. 11. Fig. 12 - 14 shows how the behaviour of this low frequency mode results in an incorrect gradients being identified by the updating procedure. Fig. 12 shows the system hinge moment response to the step input for each individual eigenvalue. The complete hinge moment response to the step input is given in Fig. 13. Fig 14 shows the hinge moment response to a sinusoidal pitch input. Both of the system responses show that the correct system response was greatly improved when applying restarting to remove the eigenvalue located at $\tilde{\Lambda} = 0.9997 + 0i$.

4.0.2 Updating complex eigenvalues

The low frequency eigenvalues of the system, can, if the low frequency response is oscillatory in nature, appear as complex conjugate pairs. A simple updating criteria weighted on the largest real eigenvalues in discrete space will fail to identify these eigenvalues. Fig 15 shows the eigenvalues for test case 1 for lift coefficient and pitch rate on the output and input channels respectively. Fig. 16 and 17 show the system response to a step down input ($\dot{\alpha} = -1$) . In the first instance we update the only discrete real eigenvalue located at $\Lambda = -0.016$. In the second instance we achieve a more favourable update by weighting the conjugate pair with the lowest frequency located at $\Lambda = 0.945 \pm 0.018$.

However care must be taken when weighting eigenvalues with nonzero imaginary parts. The very nature of these modes will exhibit oscillations depending on the damping ratio ζ given in (19). Initial investigations showed, that when using the simple updating procedure presented in this paper, the system transient response can exhibit large oscillations not present in the target (free air) solution. The oscillations were particularly large where the frequency of the updated eigenvalues were close to the the tunnel frequency (i.e. the frequency at which pressure waves are reflected back onto the aerofoil) given by [12]:

$$f_{tunnel} = \frac{2b}{\sqrt{\gamma\,(1 - M^2)}} \tag{23}$$

where f is the tunnel frequency in Hertz, $2b$ is the tunnel height, γ is the adiabatic index and M is the tunnel mach number. Clearly here more work remains to be done on the choice for the weighting sequence E_σ of the update parameter. Simply avoiding the tunnel frequencies is not a sufficient criteria to produce an update without large unwanted oscillations being introduced into the system.

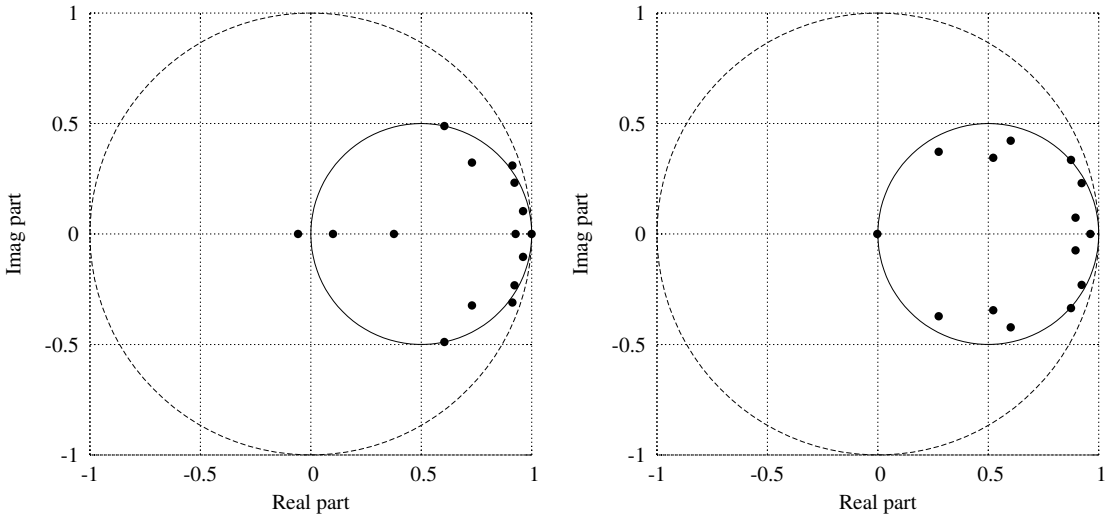

Figure 11: Eigenvalues before and after restarting (Left and Right respectively)

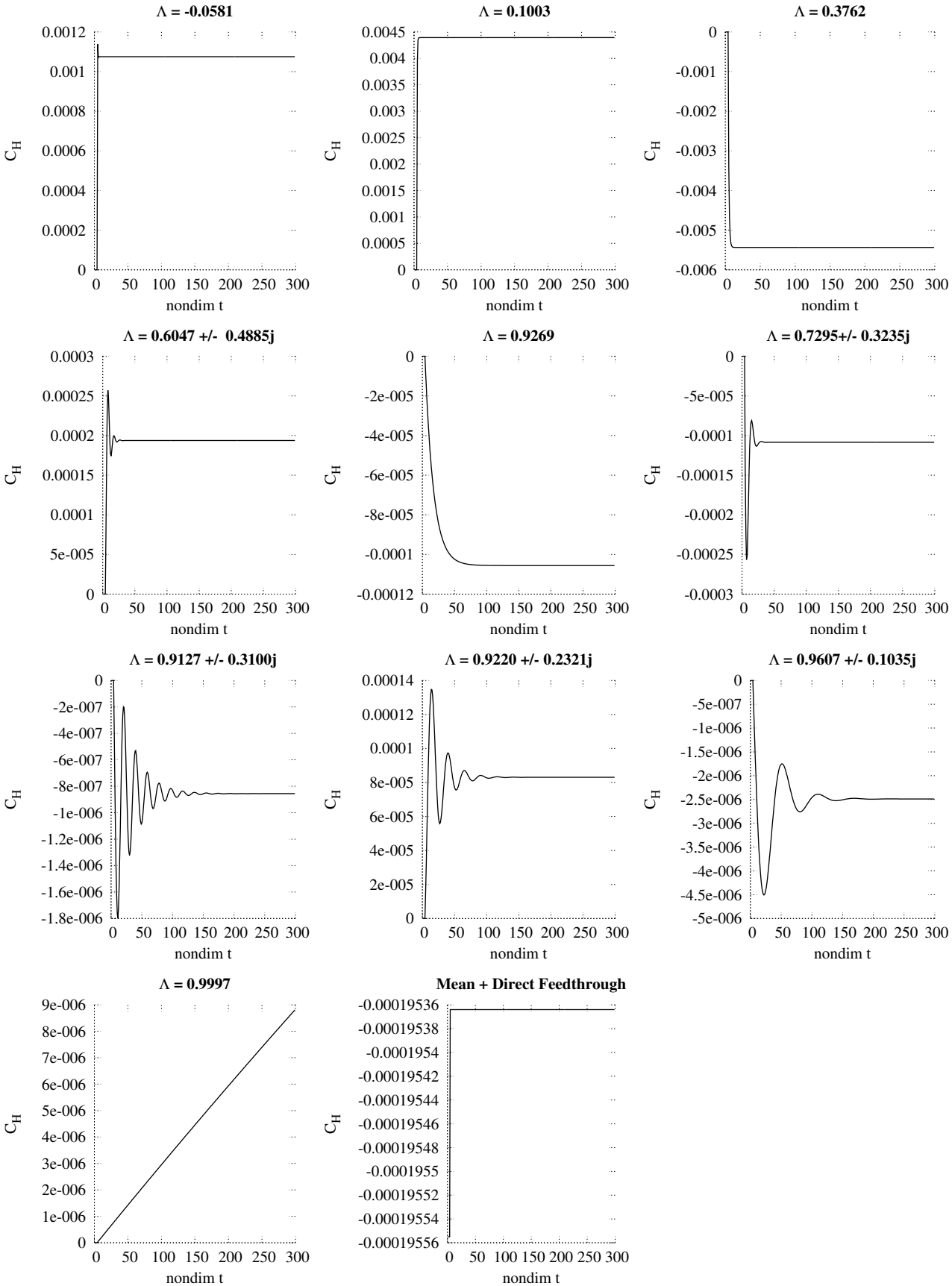

Figure 12: Hinge moment response to a step input for individual discrete eigenvalues

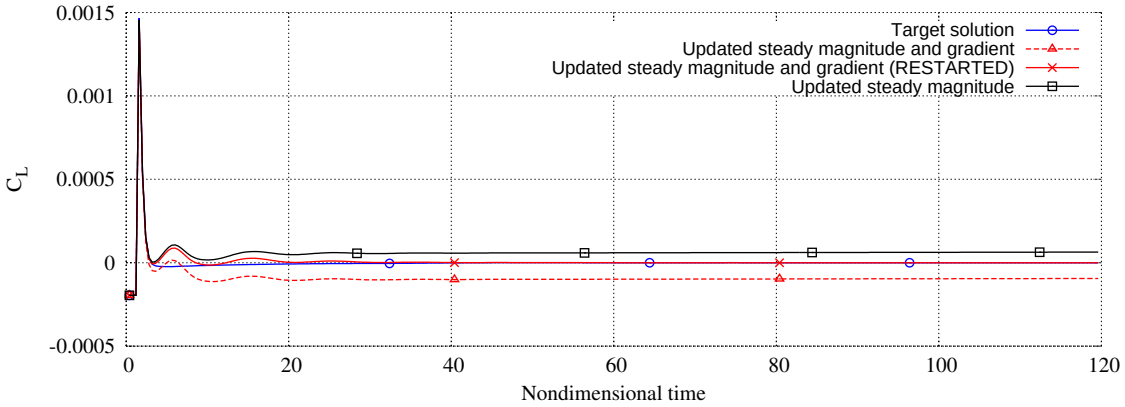

Figure 13: Hinge moment response to a step input before and after restarting

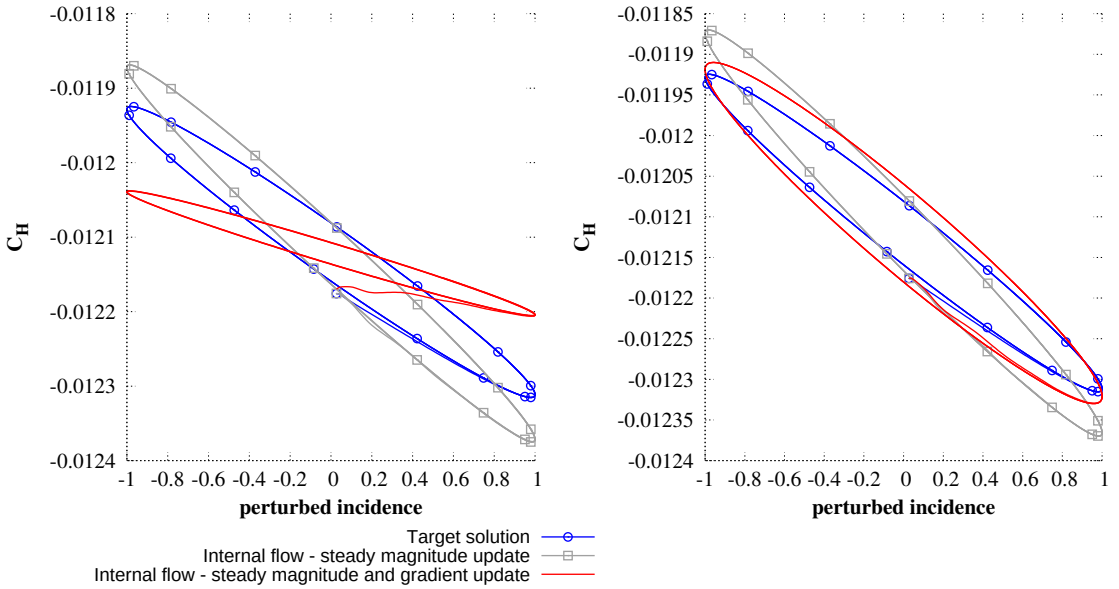

Figure 14: Hinge moment response to a sinusoidal pitch input before (left) and after (right) restarting.

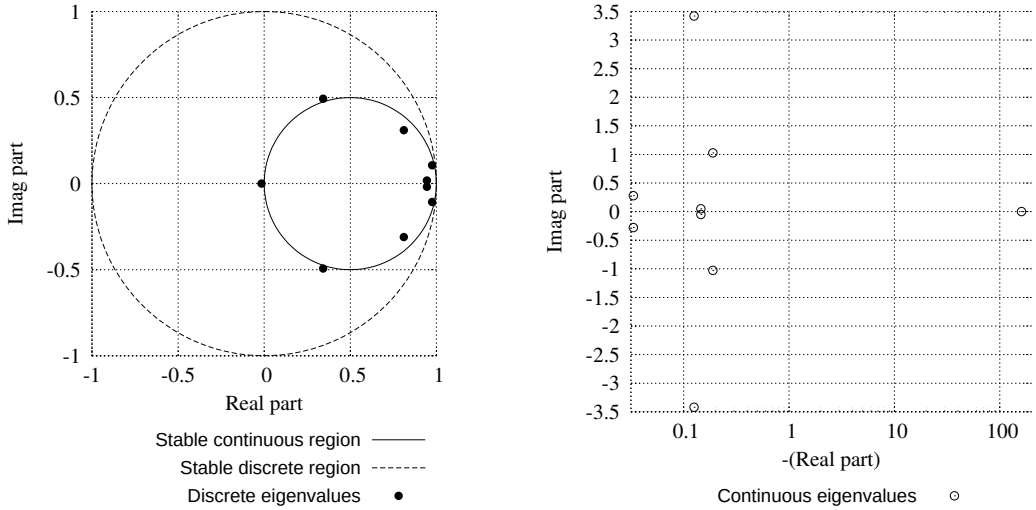

Figure 15: Eigenvalues for test case 1. ($u_i = \dot{\alpha},\ y = C_L$)

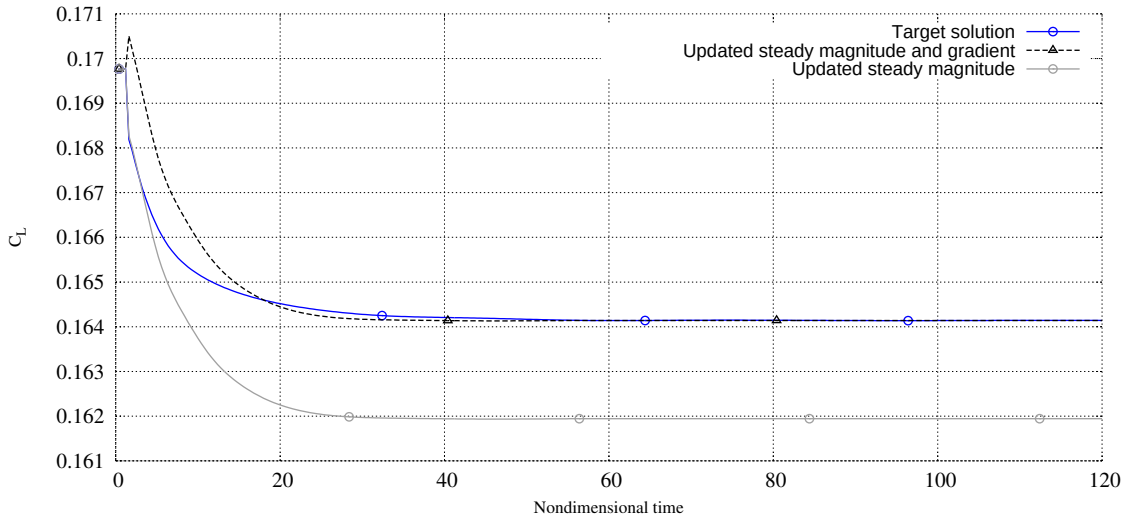

Figure 16: Response to a step input - high frequency update

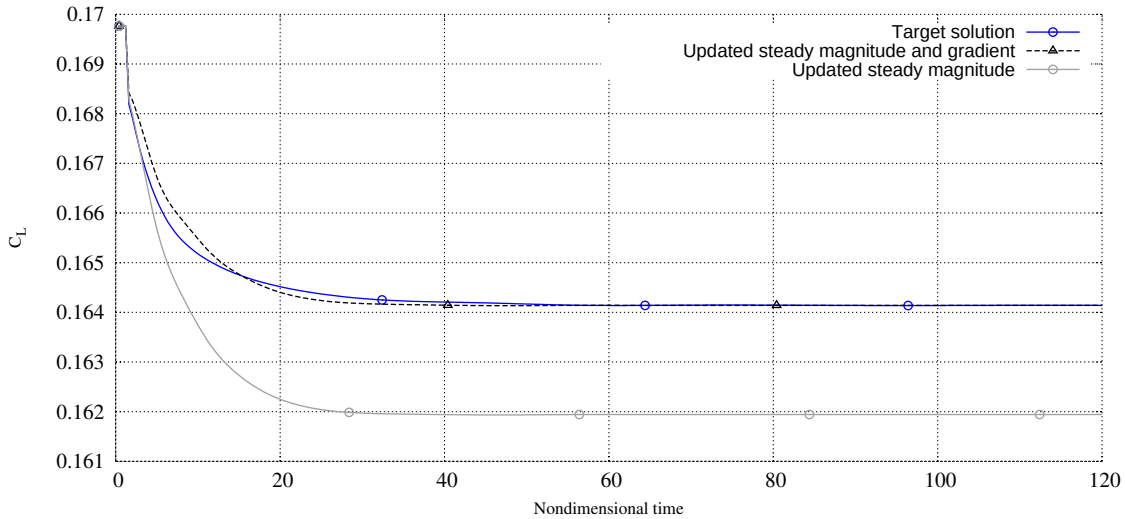

Figure 17: Response to a step input - low frequency update

5 CONCLUSIONS AND FURTHER WORK

The initial results presented here show that model updating of ROMs is a powerful tool available to the aeroelastician. The need to update the steady state gradients and the impacts this has on unsteady simulations has been demonstrated.

However, ground still remains to be covered before model updating of ROMs can be applied between any flow configurations including experimental tunnel to freestream updating procedures.

6 REFERENCES

[1] Mottershead, J. E. and Friswell, M. I. (1993). Model updating in structural dynamics: a survey. *Journal of Sound and Vibration*, 167, pp 347–375.

[2] Friswell, M. I. and Mottershead, J. E. (1995). *Finite Element Model Updating in Structural Dynamics*. Kluwer Academic Publishers.

[3] Jameson, A., Schmidt, W., and Turkel, E. (1981). Numerical solution of the euler equations by finite volume mehtodfs using runge-kutta time-stepping schemes. In *AIAA 14th Fluid and Plasma Dynamic Conference. AIAA-1981-1259.*

[4] Kroll, N. and Jain, R. K. (1987). *Solution of Two-Dimensional Euler Equations - Experience with a finite volume code.* Forschungsbericht, DFVLR-FB 87-41, Braunschweig, Germany.

[5] Gaitonde, A. L. (1994). A dual time method for the solution of the unsteady euler equations. *Aeronautical Journal*, 98, 283–291.

[6] Juang, J. and Pappa, R. S. (1985). An eigensystem realization algorithm for modal parameter identification and model reduction. *Journal of Guidance, Control, and Dynamics*, Vol 8. No. 5, 620–627.

[7] Gaitonde, A. L. and Jones, D. P. (2002). A two-dimensional linearized unsteady Euler scheme for pulse response calculations. *Proceedings of the Institution of Mechanical Engineers, Part G: Journal of Aerospace Engineering*, 216(2), 89–104. ISSN 0954-4100. doi:10.1243/095441002760179799.

[8] Silva, W. (1997). *Discrete-time linear and nonlinear aerodynamic impulse responses for efficient CFD analyses.* Ph.D. thesis, Department of Applied Science, College of William and Mary, Virginia, U.S.A.

[9] Gaitonde, A. L. and Jones, D. P. (2006). Study of linear response identification techniques and reduced-order model generation for a 2D CFD scheme. *International Journal for Numerical Methods in Fluids*, 52(12), 1361–1402. ISSN 02712091.

[10] Griffiths, L., Jones, D., and Friswell, M. (2011). Pulse input sizing for constructing reduced order models of the euler equations. In *International Forum on Aeroelasticity and structural dynamics conference.*

[11] Wales, C., Gaitonde, A., and Jones, D. (2011). Stabilisation of reduced order models via restarting. In *International Forum on Aeroelasticity and structural dynamics conference.*

[12] Ewald, B. F. R. (1998). Wind tunnel wall correction. Tech. Rep. AGARD-AG-336, AGARD.